Matsumine Hajime (Orcid ID: 0000-0001-6158-1169)

Kamei Wataru (Orcid ID: 0000-0001-7725-9123)

Niimi Yosuke (Orcid ID: 0000-0002-4203-380X)

1

Axonal supercharged interpositional jump-graft with a hybrid artificial nerve conduit containing adipose-derived stem cells in facial nerve paresis rat model

Wataru Kamei, MD,[1] Hajime Matsumine, MD, PhD,[1] Hironobu Osaki, MD, PhD,[2] Yoshifumi Ueta, PhD,[2] Satoshi Tsunoda, PhD,[1] Mari Shimizu, MD,[1] Kazuki Hashimoto, MD,[1] Yosuke Niimi, MD, PhD,[1] Mariko Miyata, MD, PhD,[2] Hiroyuki Sakurai, MD, PhD,[1]

[1] Department of Plastic and Reconstructive Surgery, Tokyo Women's Medical University, 8-1 Kawada-cho, Shinjuku-ku, Tokyo 162-8666, Japan

[2] Department of Physiology -1 (Neurophysiology), Kawada-cho, Shinjuku-ku, Tokyo 162-8666, Japan

Acknowledgement: This study was supported by JSPS KAKENHI Grant Number JP16K11382, the Hiroto Yoshioka Memorial Foundation for Medical Research, the Japan–Bangladesh Medical Association Foundation, the Toho Women's Clinic Research Foundation, the Terumo Foundation for Life Sciences and Arts, and Komei Nakayama Research scholarships.

Corresponding author: Hajime Matsumine, MD, PhD

Department of Plastic and Reconstructive Surgery, Tokyo Women's Medical University, 8-1 Kawada-cho, Shinjuku-ku, Tokyo 162-8666, Japan

Tel.: +81-3-3353-8111; Fax: +81-3-3225-0940

E-mail: matsumine@diary.ocn.ne.jp

Conflicts of Interest: None.

Axonal supercharged interpositional jump-graft with a hybrid artificial nerve conduit containing adipose-derived stem cells in facial nerve paresis rat model

Abstract

Purpose: Interpositional jump-graft (IPJG) technique with the hypoglossal nerve for supercharging can be applied in a facial nerve paresis case. In IPJG, an autologous nerve is required, and the donor site morbidity is unavoidable. Bio-degradable nerve conduits are made from polyglycolic acid (PGA) and used recently without donor site complications after providing autologous grafts. Hybrid artificial nerve conduits with adipose-derived stems cells (ASCs) also

attract attention as a nerve-regeneration enhancing agent. This study examined the effect of hybrid artificial nerve conduit on IPJG.

Materials and Methods: A total of 34 Lewis rats were used and divided into four groups by the bridge materials: autograft (n = 8), PGA nerve conduit (n = 8), hybrid PGA nerve conduit with ASCs (n = 8), and the non-treated control groups (n = 8). ASCs were collected from 2 rats and cultured. The animals were assessed physiologically and histopathologically at 13 weeks after surgery.

Results: In compound muscle action potential, the amplitude of hybrid PGA group (3,222 ± 1,779 μV) was significantly higher than that of PGA group (1,961 ± 445 μV, $p < 0.05$), and no significant difference between hybrid PGA and autograft group. All treated groups showed a myelinated nerve regeneration with double innervation in hypoglossal and facial nerve nuclei for vibrissal muscle.

Conclusion: This study showed the effectiveness of IPJG with a hybrid PGA conduit especially in physiological examination.

Running head: Interpositional jump-graft with stem cells

Keywords: Adipose-derived stems cells, Artificial nerve, Double innervation, End-to-side neurorrhaphy, Interpositional jump-graft

Introduction

Facial nerve paresis including Bell's palsy and Ramsey-Hunt syndrome appears suddenly in healthy individuals. Although remission is often focused by conservative treatment,[1] in some cases, persists paresis adversely reduced the quality of life. In these cases, the pathological mechanism involves the attenuation of central-nervous-system motor-nerve signals rather than organic damage to the facial nerves or mimetic muscles. A surgical treatment for these neuropathies is reported by May *et al*. in 1991.[2] Applying an end-to-side neurorrhaphy to the facial nerve for compensating signal attenuation with the hypoglossal nerve, they use an interpositional jump-graft (IPJG). Subsequently, many studies propose various modifications to the methodology with favorable outcomes.[3-5] End-to-side neurorrhaphy is studied by grafting the sciatic nerves to the fibular,[6] sciatic,[7] and median nerves[8] in the nerve defects of rat models. For treating the facial nerve paresis of rat model, (1) a cross-facial nerve graft method with sciatic nerve from the healthy to the paretic side of the face[9] and (2) an end-to-side loop graft method, which harvests the buccal facial-nerve branch on the healthy side and sutures the grafting nerve with nerves for creating one nerve running from the facial nerve trunk to individual branch of the facial nerve and the hypoglossal nerve,[10] are reported. These basic studies find the functional recovery of motor nerves and axonal regeneration at the neurorrhaphy site after end-to-side neurorrhaphy. Neurorrhaphy is used with favorable outcomes in clinical settings. End-to-side

sutures are used successfully from the axillary and musculocutaneous nerves to the ulnar nerve in brachial plexus palsy.[11] Facial nerve branches are reconstructed after the resection of various tumors with favorable outcomes, and the first report shows the effectiveness of loop grafts to the peripheral ends of facial nerve stumps with the sural nerve in a parotid tumor case.[12] However, the donor site morbidity is unavoidable in cases where the auricular, sural, or other nerves is taken for autologous nerve grafts. Therefore, the authors previously investigate IPJG with silicone tubes in a rat model with facial paresis and demonstrate that the efficacy of IPJG as an artificial nerve conduit.[13] However, the recovery of facial nerve paresis treated by IPJG with the nerve conduit is found to be far inferior to that of autologous nerve grafting.

On the other hand, cellular sources for inducing nerve regeneration are speculated to be stromal vascular fraction (SVF),[14] dedifferentiated fat cells,[15] basic fibroblast growth factor,[16] bone marrow stromal cells,[17] dental pulp,[18] and adipose-derived stem cells (ASCs).[19] Cells from these sources are used to promote peripheral nerve regeneration and especially, used in combination with artificial nerve conduits in research for exploring hybrid artificial nerve conduit approaches.[20] Harvesting ASCs is performed with a minimum invasiveness compared with other sources, and the harvested amount of the cells is easily increased. Therefore, ASCs are believed to be a potentially and clinically applicable cell source. Favorable outcomes are reported on ASC clinical applications for treating Crohn's fistula,[21] graft-versus-host disease,[22] and stress urinary incontinence,[23] and for cosmetic breast alteration surgery.[24]

For obtaining IPJGs, of which functions are closely resembles those of autologous nerve grafts, this study constructed a hybrid artificial nerve conduit with ASCs as an IPJG and evaluated the effectiveness of ASCs in the conduits for end-to-side neurorrhaphy histopathologically and physiologically.

Materials and Methods

All animal care and handling procedures were performed in accordance with the Principles of Laboratory Animal Care of Tokyo Women's Medical University Animal Experimentation Committee. Thirty-four male syngeneic Lewis rats were obtained from Charles River Laboratories Japan (Tokyo, Japan) and used through this study.

Preparation of ASCs and Hybrid Polyglycolic Acid-based Tube

Two-eight-week-old male rats were used. Adipose tissue was collected from the inguinal region of the animal and washed with phosphate-buffered saline (PBS) (Thermo Fisher Scientific, Carlsbad, CA, USA). Cells were then isolated mechanically from the tissue and treated with 0.075% collagenase type I (Thermo Fisher Scientific) at 37 °C for 30 min, filtered through 70-μm cell strainers (BD Falcon, Becton Dickinson, Oxford, UK), neutralized by adding Dulbecco's minimum essential medium (DMEM) (Thermo Fisher Scientific) containing 10% fetal bovine serum (FBS), and centrifuged at 800 × g for 5 min. Precipitated stromal cells were

re-cultured in a 100-mm tissue culture dish at 37 °C in 5% CO_2. At 24 h after the initiation of culture, non-adherent supernatant was removed, and the medium was exchanged with fresh medium. Cells were cultured adherently for 1 to 2 weeks at 37 °C in 5% CO_2 with medium change every 72 h. After reaching to approximately 80% confluence, cells were detached enzymatically with 0.25% trypsin solution and passaged in fresh medium. A total of 1×10^5 cultured cells were obtained at passage number two (P2) and put into a polyglycolic acid (PGA) tube (Nerbridge) (Toyobo, Osaka, Japan) with 10 μL type 1 collagen solution (Fig. 1).

ASCs as Mesenchymal Stem Cells

ASCs showed a self-propagation ability with a flattened fibroblast morphology at P2 (Fig.2A) and were labeled with mouse monoclonal anti-Stro-1 antibody (MAB1038) (R&D Systems, Minneapolis, MN), a mesenchymal stem cell (MSC) marker (Fig. 2B).

Experimental Design

The rats were divided into four groups. The rats belonging to the autograft group (n = 8), the PGA group (n = 8), and the hybrid PGA group (n = 8) underwent IPJG with an ipsilateral great auricular nerve, PGA tube, and PGA tube containing ASCs, respectively, and the non-treatment rats became the control group (n = 8). Histopathological and physiological assessments were performed at 13 weeks postoperatively.

Surgical Procedure

Rats were anesthetized with 3% isoflurane with an inhalation anesthesia apparatus (KN–1071 NARCOBIT-E) (Natsume Seisakusho, Tokyo). After the rat was kept in a right lateral recumbent position, an S-shaped incision was made extending from behind the left ear to the lower margin of the ipsilateral mandible (Fig. 3A). The great auricular nerve was identified on the sternocleidomastoid muscle approximately 10 mm ventral to the posterior auricular surface. Dissection was advanced above the sternocleidomastoid muscle, and the facial nerve trunk was identified emerging from the anterior margin of the sternocleidomastoid muscle. The external jugular vein was then ligatured and transected, and the digastricus was identified. Dissection was advanced deeply into the digastricus, and the hypoglossal nerve was identified (Fig. 3B). For preparing a rat facial nerve paresis model as reported by Shichinohe *et al*.,[25] a ligature clip (LIGACLIP MCA, Ethicon, OH) was allowed to crush the facial nerve trunk (Fig. 3C). Subsequently, the procedures were completed for all groups. A 7-mm section was harvested from the ipsilateral great auricular nerve and used as IPJG to make the autograft group (Fig. 3D). A 10-mm PGA tube was used as IPJG to make PGA group (Fig. 3E). A 10-mm hybrid PGA tube containing ASCs was used as IPJG to make hybrid PGA group (Fig. 3F). A 1.5-mm slit was made at both ends of artificial nerve conduit for inserting hypoglossal and facial nerves into the slits individually in PGA and hybrid PGA groups, and a 7-mm nerve bridge was expected to

appear in the conduit. End-to-side neurorrhaphy was performed with an epineural window on the facial or hypoglossal neve. As the control group, rats were underwent no further treatment after the facial nerve trunk was crushed with a ligature clip. Surgery was performed with a microscope (M60) (Leica Microsystems, Wetzlar, Germany).

Compound Muscle Action Potential (CMAP) Measurement with Vibrissal Muscles

For assessing the functions of regenerated nerves, CMAP was measured. The depth of anesthesia was confirmed by observing the disappearance of eyelid reflex and the absence of whisker movement. CMAP was measured at two sites per rat, and the mean value was obtained from 10 successive stimulation pulses. Amplitude, duration, and latency were measured, and these parameters were measured with custom-made MATLAB software (MathWorks, Natick, MA).

Retrograde Fluorescence Tracing of Facial and Hypoglossal Motor Nuclei

Retrograde fluorescence tracers DiI (D-28) and DiO (D-275) (Invitrogen, Carlsbad, CA) were injected into the left whisker pads and tongue of rats at 11 weeks postoperatively to evaluate double innervation. Rats were anaesthetized with 4% isoflurane via the inhalation apparatus and injected with 100 μL 1% DiI in ethanol and 200 μL 0.5% DiO in N,N-dimethylformamide with a 25-μL Hamilton syringe (Hamilton, Reno, NV). Two weeks later, rats were euthanized under

deep anesthesia, and whole animal perfusion fixation was performed. The thorax and abdomen were incised, and 150 mL of 0.1 mol/L PBS was injected into the left ventricle, followed by 300 mL of 4% paraformaldehyde. The brain was extirpated and fixed with 4% paraformaldehyde and 0.2% picric acid for at least 1 day. Subsequently, 50-μm-thick coronal sections were prepared from the brain stem with a vibratome (VT1000S) (Leica Microsystems, Buffalo Grove, IL). For preparing specimens, sections were treated with 0.005% DAPI solution in the dark for 5 min and washed again with 0.1 mol/L PBS, mounted on gelatin-coated glass slides, and cover-slipped with aqueous mounting medium. Sections were then examined with a cooled charged-coupled device (CCD) camera (Quantum Scientific Imaging, Poplarville, MS) for observing DiI, DiO, and DAPI fluorescence signals.

Toluidine Blue Staining of Regenerated Nerves

After CMAP measurement, the central part of the nerve graft was harvested and fixed serially with 2% paraformaldehyde, 2% glutaraldehyde, and then overnight in 0.1 mol/L cacodylate buffer solution at pH 7.4 at 4 °C. Nerve specimens were washed, post-fixed with 2% osmium tetroxide, then dehydrated with ethanol, which was replaced with propylene oxide, embedded in resin (Quetol-812) (Nisshin EM, Tokyo). The specimen-embedded resin was allowed to polymerize for 48 h at 60 °C. After complete polymerization, 1.5-μm sections were prepared from the resin with an ultramicrotome (Ultracut UCT) (Leica, Vienna, Austria) and stained with

toluidine blue. The sliced specimens were photographed with a microscope (Leica DM ILLED) (Leica). Regenerated nerves found in photographs were counted by Photoshop CC 2017 (Adobe Systems, San Jose, CA).

Electron Microscopic Examination of Regenerated Nerves

Ultra-thin sections with a thickness of 70 nm were prepared from resin-embedded specimens with the ultramicrotome with a diamond knife. Sections were stained with 2% uranyl acetate for 15 min at room temperature, washed with distilled water, and stained with lead stain solution (Sigma-Aldrich, St. Louis, MO) for 3 min. A JEM-1400Plus electron microscope (JEOL, Tokyo) was used at an acceleration voltage of 80 kV. Digital images were taken with a CCD camera (EM-14830RUBY2) (JEOL). Fiber diameter, axon diameter, and myelin thickness were measured at five randomly selected sites by Photoshop CC 2017.

Statistical Analysis

Mean values and standard deviations were calculated for data obtained from CMAP measurements, toluidine blue staining, and electron microscopy. P values less than 0.05 ($p < 0.05$) were considered significant. Data from individual groups were analyzed with analysis of variance (ANOVA) and Tukey's multiple comparison test, using JMP® software, version 13 (SAS Institute, Cary, NC).

Results

All rats survived after surgery, and no animal showed any complications. Autograft, PGA, and hybrid PGA groups showed macroscopic nerve regeneration at 13 weeks postoperatively (Fig. 4A, B, and C). Toluidine blue stained specimens revealed myelin sheath and axonal regeneration in autograft (Fig.4D), PGA (Fig.4E), and hybrid PGA groups (Fig.4F). Distinct dense nerve regeneration was observed in the autograft group compared with PGA and hybrid PGA groups. Electron microscopy revealed myelinated nerve regeneration in the autograft (Fig. 5A), PGA (Fig. 5B), and hybrid PGA groups (Fig. 5C). Mean number of regenerated myelinated fibers of autograft group (1,852 ± 365) was significantly higher than those of other two IPJG treatment groups ($p < 0.01$); hybrid PGA group (320 ± 210) and PGA group (177 ± 78) (Fig. 6A).

Mean nerve fiber diameter of autograft group (5.7 ± 2.2 μm) (Fig. 6B) was significantly higher than those of PGA (4.5 ±0.2 μm) ($p < 0.01$) and hybrid PGA groups (5.0 ±2.2 μm) ($p < 0.05$).

No significant differences in axon diameter (Fig. 6C) were found among autograft (4.2 ± 1.8 μm), PGA (3.6 ± 2.0 μm), and hybrid PGA groups (3.6 ± 1.9 μm).

Myelin thickness of autograft group (0.79 ± 0.03 μm) was significantly higher than that of hybrid PGA group (0.68 ± 0.29 μm) ($p < 0.01$), and that of hybrid PGA group was significantly higher than that of PGA group (0.44 ± 0.03 μm) ($p < 0.01$) (Fig. 6D).

The g ratio (axon/fiber diameter ratio) of PGA group (0.80 ± 0.15) ($p < 0.01$) was significantly higher than those of autograft and hybrid PGA groups (Fig. 6E).

CMAP measurement revealed muscle contractions after stimulation in all groups (Fig. 7A-D). Amplitude was greatest in autograft group (4,352 ± 1,587 μV), followed by hybrid PGA (3,222 ± 1,779 μV), PGA (1,961 ± 445 μV), and the control groups (687 ± 490 μV) (Fig. 7E). The amplitude of hybrid PGA group was found to be significantly higher than that of PGA group. Duration of PGA group (0.49 ± 0.14 ms) was shortest among other groups; hybrid PGA (0.52 ± 0.14 ms), autograft (0.95 ± 0.68 ms), and the control groups (1.11 ± 0.53 ms) (Fig. 7F). Duration values of PGA and hybrid PGA groups were significantly shorter than those of the control and autograft groups ($p < 0.05$). Latency was shortest in the autograft group (2.8 ± 0.9 ms), followed by hybrid PGA (4.3 ± 1.7 ms), the control (4.4 ± 0.4 ms), and PGA group (6.6 ± 2.8 ms) (Fig. 7G). Latency was significantly shorter in hybrid PGA than PGA groups ($p < 0.01$).

Retrograde tracer examinations revealed DiI and DiO-positive motor neurons in both facial nerve nuclei (7N) and hypoglossal nuclei (12N) in the control group (Fig. 8A and B). On the other hand, autograft, PGA, and hybrid PGA groups, DiI and DiO-positive motor neurons were observed in both 7N and 12N with double innervation (Fig.8C-J), indicating that the double innervation of mimetic muscles in 7N and 12N.

Discussion

Although the histopathological results of this study showed that the number of myelinated fibers of hybrid PGA group was unable to reach to that of autograft group, and the regenerated axonal thickness of hybrid PGA was comparable to that of autograft group, and the thickness of the myelin sheath was thicker than that of PGA group. The physiological results by CMAP showed that hybrid PGA-treated rats showed a significantly greater amplitude value than PGA-treated rats, and the amplitude value was comparable to that of autograft rats. These results demonstrated that ASCs in conduits promoted nerve regeneration and thicker myelin-sheath formation after nerve conduits bridged nerves by end-to-side neurorrhaphy. ~~Especially, physiological examination was considered to show a clinical significance that the nerve regeneration of hybrid PGA group was similar with that of the autograft group.~~ Although the number of regenerated myelinated fibers of the hybrid PGA group was lower than that of the autograft group, in the g-ratio representing the axonal myelination,[26] there was no significant difference between these two groups, indicating that the quality of the regenerated nerve of the hybrid PGA group was comparable to that of the autograft group.

The retrograde results proved that end-to-side neurorrhaphy allowed regenerated nerves to have double innervation by functional facial and hypoglossal nerve neurons. Previously, experiments on retrograde tracers from whisker pads and tongues are performed in a model similar to that of this study for investigating interactive nerve regeneration.[13,27] Referring the results of the

references, the authors speculated that this study's model also proved no facial complete paralysis, indicating that IPJG provided double innervation to the mimetic muscles.

Previously, hybrid artificial nerve conduits containing ASCs are investigated in rats with sciatic nerve deficit.[28] Although ASCs are unable to survive through 2 weeks after transplantation, they are considered to promote nerve regeneration by secreting neurotrophic factors such as nerve growth factor (NGF),[29] brain-derived neurotrophic factor (BDNF)[30] and vascular endothelial growth factor (VEGF)[31] in the early post-transplant period. ASCs reportedly transform into Schwann-like cells with exudate released from damaged sciatic nerve in rats,[32] and the transformation was considered to be performed by secreted NGF, BDNF, and neurotrophin 3 from healthy Schwann cells in the deficient nerve. Therefore, the mechanism of ASC-promoted nerve regeneration in this study might consist of two serial paracrine actions; (1) the release of neurotrophic factors from the grafted ASCs in artificial nerve conduit and (2) the transformation of ASCs into Schwann-like cells with released neurotrophic factors from facial and hypoglossal nerves at the host sites where epineural windows were made by end-to-side neurorrhaphy.

These experimental models were incomplete paralysis models and suitable for investigating the efficacy of neural supercharging from the hypoglossal nerve to the facial nerve, because IPJG procedure is a technique for an incomplete facial paralysis in clinical cases. Classical IPJG technique contains the axotomy of the hypoglossal nerve. However, the subsequent development of basic research on end-to-side neurorrhaphy highlights new techniques such as the

fenestrations of the epineurium and the perineurium, and end-to-side neurorrhaphy without the host-site axotomy. Nerve fiber influx is observed in the regenerated nerves treated by these techniques.[33,34] Axotomy is reported to promote collateral spouting.[35] In this study, epineural windows were made by a technique similar to IPJG method reported by Ueda *et al*.,[5] because the technique could avoid damaging the functions of the residual facial nerves, or the hypoglossal nerve, which are known to be the source of supercharging. Therefore, this study performed neurorrhaphy with the technique meticulously for reducing the risk of axonal damage. Since the murine hypoglossal nerve lies deeply within the cervical region and end-to-side neurorrhaphy with a 1-mm diameter artificial conduit could be difficult, this study was able to successfully perform the procedure with untied sutures for both the hypoglossal nerve and facial nerve sides. Further studies including an investigation on differences in nerve regeneration between axotomy and non-axotomy groups and investigations on comorbidities such as the atrophy of the tongue were required.

This study performed a 7-mm IPJG in a rat facial nerve paresis model and obtained favorable outcomes in hybrid PGA group. However, a nerve bridge of around 50 to 70 mm in length will be required in clinical use. Currently, there is no data showing the size of nerve deficit where a hybrid conduit is effective. Future research using larger experimental animals with longer artificial nerve conduits is needed to confirm the limit of the range where regeneration can be achieved. This is the first report of end-to-side nerve neurorrhaphy with hybrid artificial nerve

conduits containing ASCs. ~~Although the regeneration of myelinated fibers within the central part of the graft in all treatment groups was observed, the morphological data of the buccal branch including the control group was important in the recovery of facial nerve paresis. Collecting no buccal branch in this study, the authors will consider collecting the buccal branch in the future study.~~ The regeneration of myelinated fibers within the central part of the graft in all treatment groups was observed, and these morphological data indicated that ASCs promoted nerve regeneration even in the artificial nerve conduits, which was used end-to-side neurorrhaphy.

Conclusion

This study successfully demonstrated end-to-side neurorrhaphy for the facial and hypoglossal nerves with a hybrid PGA nerve conduit containing ASCs, which promote nerve regeneration for the neurorrhaphy. This study clarified that the technique could potentially come closer to conventional IPJG techniques with autologous grafts.

1. Campbell ED, Hickey RP, Nixon KH, Richardson AT. Value of nerve-excitability measurements in prognosis of facial palsy. Br Med J 1962;2(5296):7-10.
2. May M, Sobol SM, Mester SJ. Hypoglossal-facial nerve interpositional-jump graft for facial reanimation without tongue atrophy. Otolaryngol Head Neck Surg 1991;104(6):818-825.

3. Yamamoto Y, Sekido M, Furukawa H, Oyama A, Tsutsumida A, Sasaki S. Surgical rehabilitation of reversible facial palsy: facial--hypoglossal network system based on neural signal augmentation/neural supercharge concept. J Plast Reconstr Aesthet Surg 2007;60(3):223-231.
4. Yoleri L, Songur E, Yoleri O, Vural T, Cagdas A. Reanimation of early facial paralysis with hypoglossal/facial end-to-side neurorrhaphy: a new approach. J Reconstr Microsurg 2000;16(5):347-355; discussion 355-346.
5. Ueda K, Akiyoshi K, Suzuki Y, Ohkouchi M, Hirose T, Asai E, Tateshita T. Combination of hypoglossal-facial nerve jump graft by end-to-side neurorrhaphy and cross-face nerve graft for the treatment of facial paralysis. J Reconstr Microsurg 2007;23(4):181-187.
6. Viterbo F, Trindade JC, Hoshino K, Mazzoni Neto A. Latero-terminal neurorrhaphy without removal of the epineural sheath. Experimental study in rats. Rev Paul Med 1992;110(6):267-275.
7. Lundborg G, Zhao Q, Kanje M, Danielsen N, Kerns JM. Can sensory and motor collateral sprouting be induced from intact peripheral nerve by end-to-side anastomosis? J Hand Surg Br 1994;19(3):277-282.
8. Hayashi A, Yanai A, Komuro Y, Nishida M, Inoue M, Seki T. Collateral sprouting occurs following end-to-side neurorrhaphy. Plast Reconstr Surg 2004;114(1):129-137.

9. Matsuda K, Kakibuchi M, Kubo T, Tomita K, Fujiwara T, Hattori R, Yano K, Hosokawa K. A new model of end-to-side nerve graft for multiple branch reconstruction: end-to-side cross-face nerve graft in rats. J Plast Reconstr Aesthet Surg 2008;61(11):1357-1367.

10. Matsumine H, Sasaki R, Takeuchi Y, Watanabe Y, Niimi Y, Sakurai H, Miyata M, Yamato M. Unilateral Multiple Facial Nerve Branch Reconstruction Using "End-to-side Loop Graft" Supercharged by Hypoglossal Nerve. Plast Reconstr Surg Glob Open 2014;2(10):e240.

11. Haninec P, Mencl L, Kaiser R. End-to-side neurorrhaphy in brachial plexus reconstruction. J Neurosurg 2013;119(3):689-694.

12. Kakibuchi M, Tuji K, Fukuda K, Terada T, Yamada N, Matsuda K, Kawai K-i, Sakagami M. End-to-Side Nerve Graft for Facial Nerve Reconstruction. Ann Plast Surg 2004;53(5):496-500.

13. Niimi Y, Matsumine H, Takeuchi Y, Sasaki R, Watanabe Y, Yamato M, Miyata M, Sakurai H. Effectively Axonal-supercharged Interpositional Jump-Graft with an Artificial Nerve Conduit for Rat Facial Nerve Paralysis. Plast Reconstr Surg Glob Open 2015;3(6):e416.

14. Matsumine H, Numakura K, Climov M, Watanabe Y, Giatsidis G, Orgill DP. Facial-nerve regeneration ability of a hybrid artificial nerve conduit

containing uncultured adipose-derived stromal vascular fraction: An experimental study. Microsurgery 2016;37(7):808-818.

15. Matsumine H, Takeuchi Y, Sasaki R, Kazama T, Kano K, Matsumoto T, Sakurai H, Miyata M, Yamato M. Adipocyte-derived and dedifferentiated fat cells promoting facial nerve regeneration in a rat model. Plast Reconstr Surg 2014;134(4):686-697.
16. Matsumine H, Sasaki R, Tabata Y, Matsui M, Yamato M, Okano T, Sakurai H. Facial nerve regeneration using basic fibroblast growth factor-impregnated gelatin microspheres in a rat model. J Tissue Eng Regen Med 2014;10(10):E559-E567.
17. Dezawa M, Takahashi I, Esaki M, Takano M, Sawada H. Sciatic nerve regeneration in rats induced by transplantation of in vitro differentiated bone-marrow stromal cells. Eur J Neurosci 2001;14(11):1771-1776.
18. Sasaki R, Matsumine H, Watanabe Y, Takeuchi Y, Yamato M, Okano T, Miyata M, Ando T. Electrophysiologic and functional evaluations of regenerated facial nerve defects with a tube containing dental pulp cells in rats. Plast Reconstr Surg 2014;134(5):970-978.
19. Watanabe Y, Sasaki R, Matsumine H, Yamato M, Okano T. Undifferentiated and differentiated adipose-derived stem cells improve nerve regeneration in a rat model of facial nerve defect. J Tissue Eng Regen Med 2014;11(2):362-374.

20. Hu F, Zhang X, Liu H, Xu P, Doulathunnisa, Teng G, Xiao Z. Neuronally differentiated adipose-derived stem cells and aligned PHBV nanofiber nerve scaffolds promote sciatic nerve regeneration. Biochem Biophys Res Commun 2017;489(2):171-178.

21. Garcia-Olmo D, Garcia-Arranz M, Herreros D, Pascual I, Peiro C, Rodriguez-Montes JA. A phase I clinical trial of the treatment of Crohn's fistula by adipose mesenchymal stem cell transplantation. Dis Colon Rectum 2005;48(7):1416-1423.

22. Fang B, Song Y, Lin Q, Zhang Y, Cao Y, Zhao RC, Ma Y. Human adipose tissue-derived mesenchymal stromal cells as salvage therapy for treatment of severe refractory acute graft-vs.-host disease in two children. Pediatr Transplant 2007;11(7):814-817.

23. Yamamoto T, Gotoh M, Kato M, Majima T, Toriyama K, Kamei Y, Iwaguro H, Matsukawa Y, Funahashi Y. Periurethral injection of autologous adipose-derived regenerative cells for the treatment of male stress urinary incontinence: Report of three initial cases. Int J Urol 2012;19(7):652-659.

24. Yoshimura K, Sato K, Aoi N, Kurita M, Hirohi T, Harii K. Cell-assisted lipotransfer for cosmetic breast augmentation: supportive use of adipose-derived stem/stromal cells. Aesthetic Plast Surg 2008;32(1):48-55; discussion 56-47.

25. Shichinohe R, Furukawa H, Sekido M, Saito A, Hayashi T, Funayama E, Oyama A, Yamamoto Y. Direction of innervation after interpositional nerve graft between facial and hypoglossal nerves in individuals with or without facial palsy: a rat model for treating incomplete facial palsy. J Plast Reconstr Aesthet Surg 2012;65(6):763-770.

26. Chomiak T, Hu B. What is the optimal value of the g-ratio for myelinated fibers in the rat CNS? A theoretical approach. PLoS One 2009;4(11):e7754.

27. Niimi Y, Matsumine H, Takeuchi Y, Osaki H, Tsunoda S, Miyata M, Yamato M, Sakurai H. A collagen-coated PGA conduit for interpositional-jump graft with end-to-side neurorrhaphy for treating facial nerve paralysis in rat. Microsurgery 2018.

28. Erba P, Mantovani C, Kalbermatten DF, Pierer G, Terenghi G, Kingham PJ. Regeneration potential and survival of transplanted undifferentiated adipose tissue-derived stem cells in peripheral nerve conduits. J Plast Reconstr Aesthet Surg 2010;63(12):e811-817.

29. Peeraully MR, Jenkins JR, Trayhurn P. NGF gene expression and secretion in white adipose tissue: regulation in 3T3-L1 adipocytes by hormones and inflammatory cytokines. Am J Physiol Endocrinol Metab 2004;287(2):E331-339.

30. Wei X, Du Z, Zhao L, Feng D, Wei G, He Y, Tan J, Lee WH, Hampel H, Dodel R, Johnstone BH, March KL, Farlow MR, Du Y. IFATS collection: The conditioned

media of adipose stromal cells protect against hypoxia-ischemia-induced brain damage in neonatal rats. Stem Cells 2009;27(2):478-488.

31. Sondell M, Lundborg G, Kanje M. Vascular endothelial growth factor has neurotrophic activity and stimulates axonal outgrowth, enhancing cell survival and Schwann cell proliferation in the peripheral nervous system. J Neurosci 1999;19(14):5731-5740.

32. Liu Y, Zhang Z, Qin Y, Wu H, Lv Q, Chen X, Deng W. A new method for Schwann-like cell differentiation of adipose derived stem cells. Neurosci Lett 2013;551:79-83.

33. Viterbo F, Trindade JC, Hoshino K, Mazzoni A. Two end-to-side neurorrhaphies and nerve graft with removal of the epineural sheath: experimental study in rats. Br J Plast Surg 1994;47(2):75-80.

34. Matsumoto M, Hirata H, Nishiyama M, Morita A, Sasaki H, Uchida A. Schwann cells can induce collateral sprouting from intact axons: experimental study of end-to-side neurorrhaphy using a Y-chamber model. J Reconstr Microsurg 1999;15(4):281-286.

35. Hayashi A, Pannucci C, Moradzadeh A, Kawamura D, Magill C, Hunter DA, Tong AY, Parsadanian A, Mackinnon SE, Myckatyn TM. Axotomy or compression is required for axonal sprouting following end-to-side neurorrhaphy. Exp Neurol 2008;211(2):539-550.

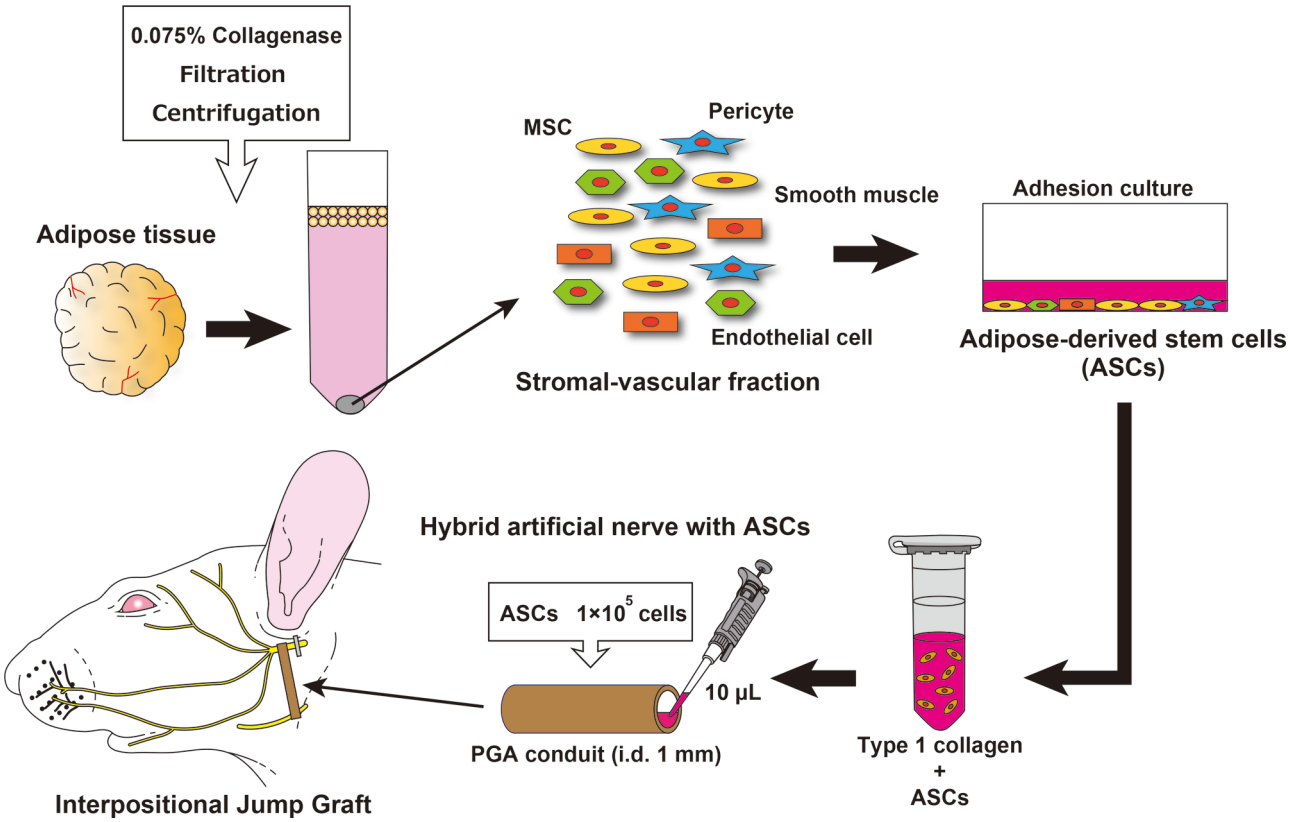

micr-18-0014-File003.tif

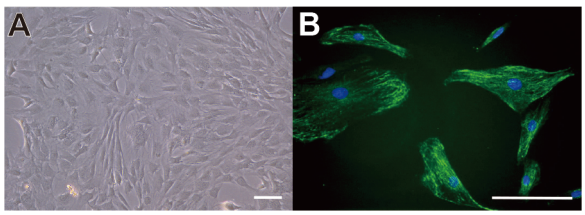

micr-18-0014-File004.tif

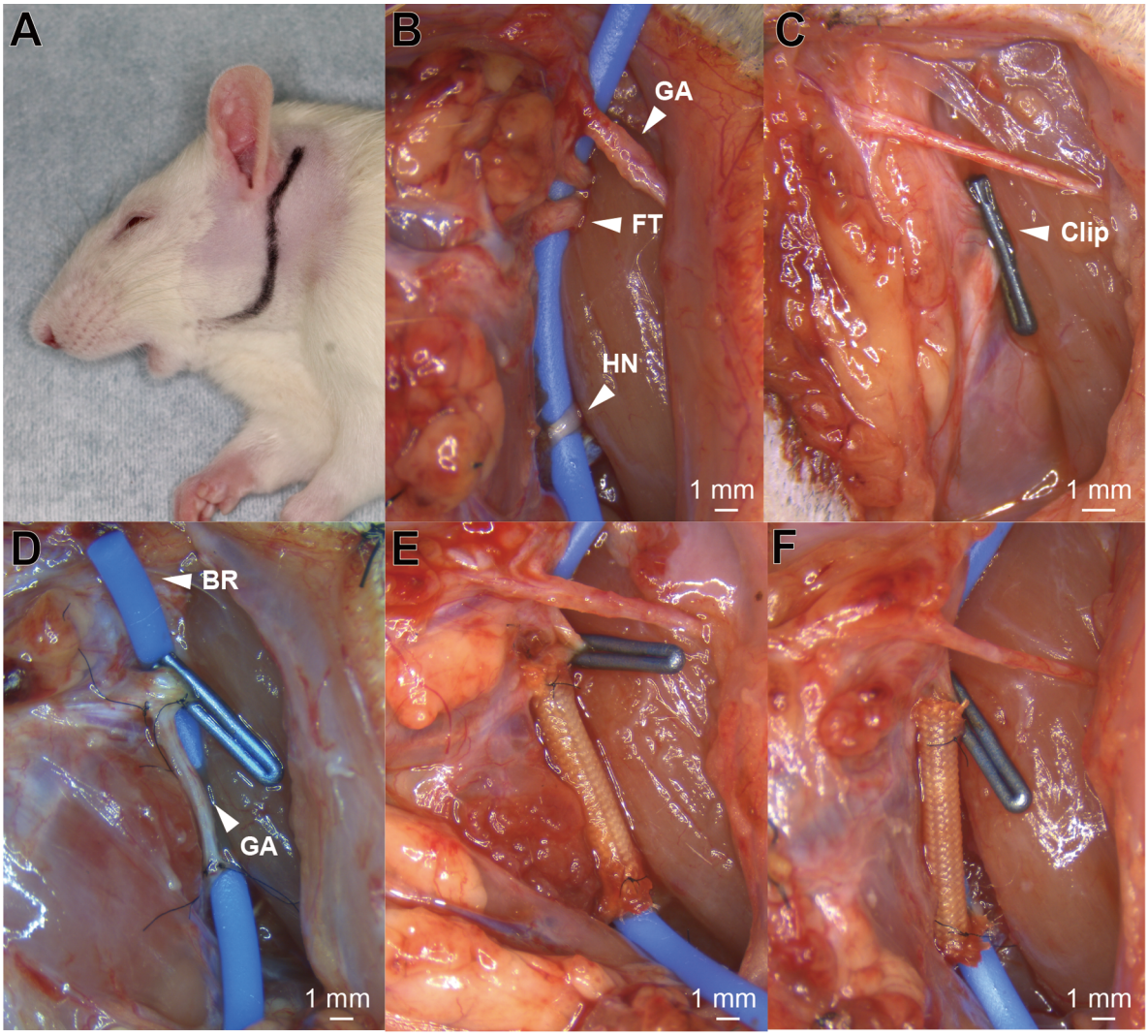

micr-18-0014-File005.tif

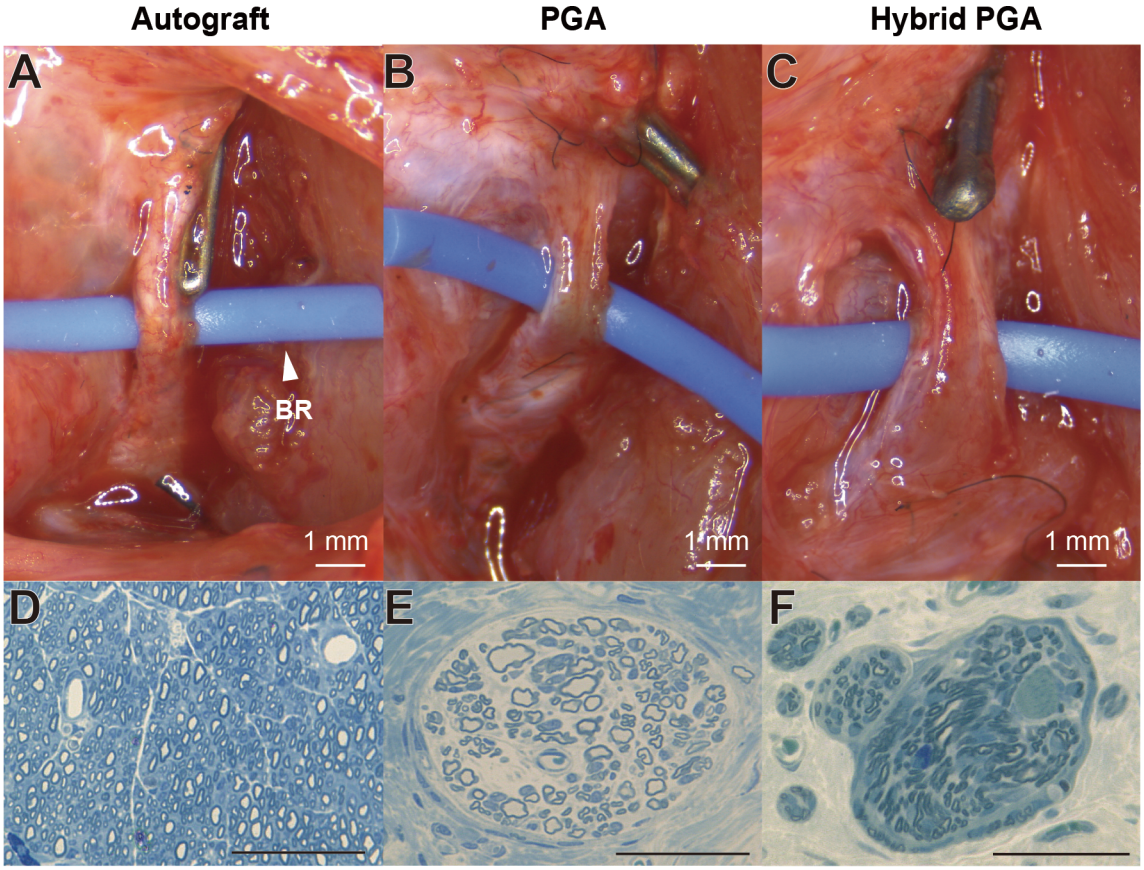

micr-18-0014-File006.tif

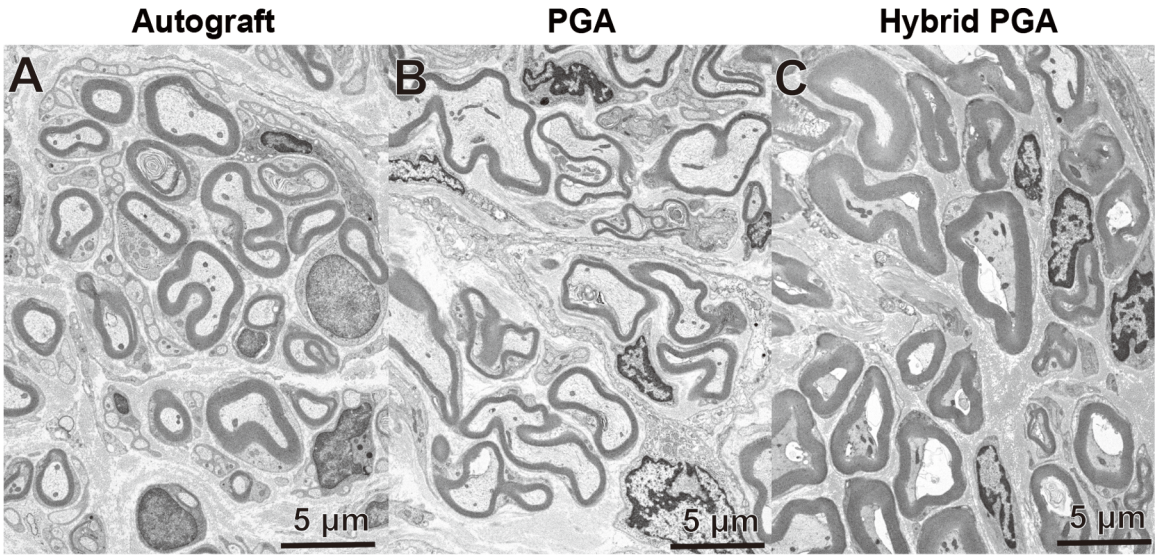

micr-18-0014-File007.tif

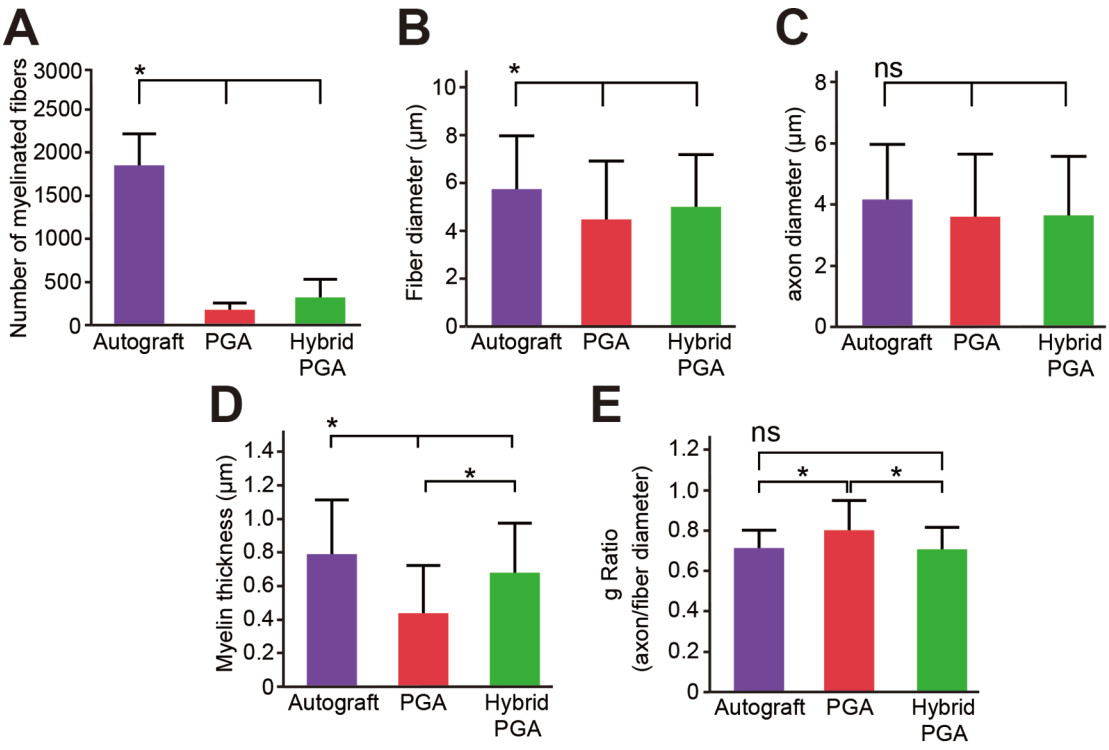

micr-18-0014-File008.tif

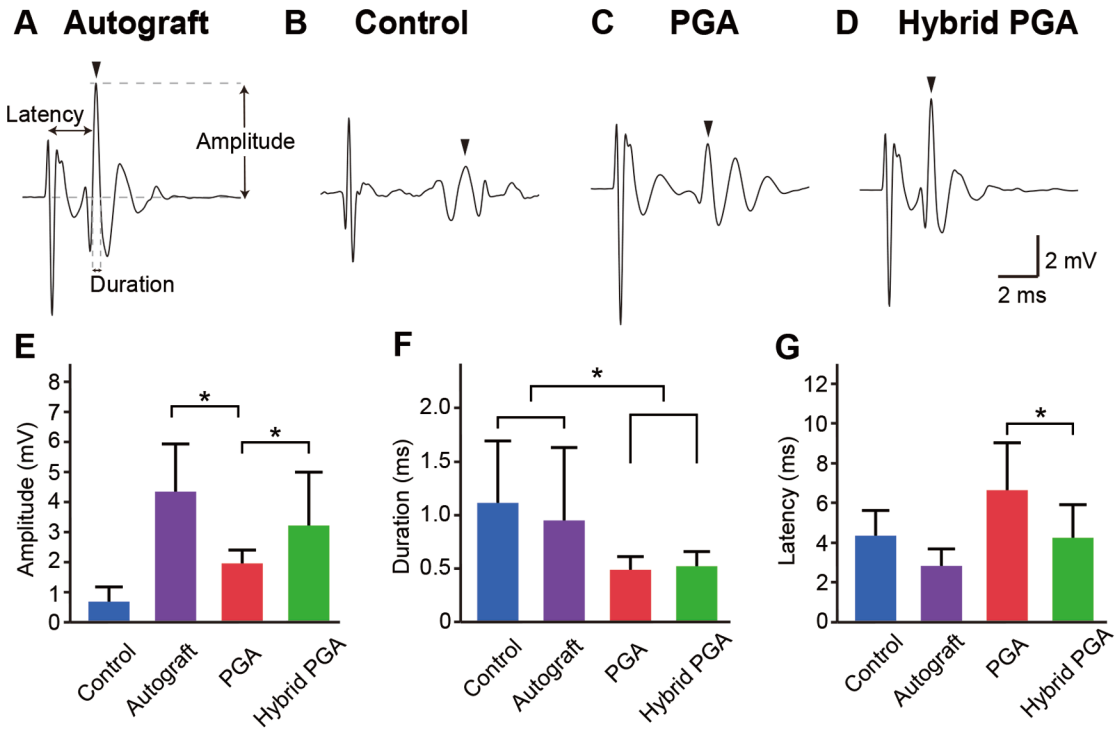

micr-18-0014-File009.tif

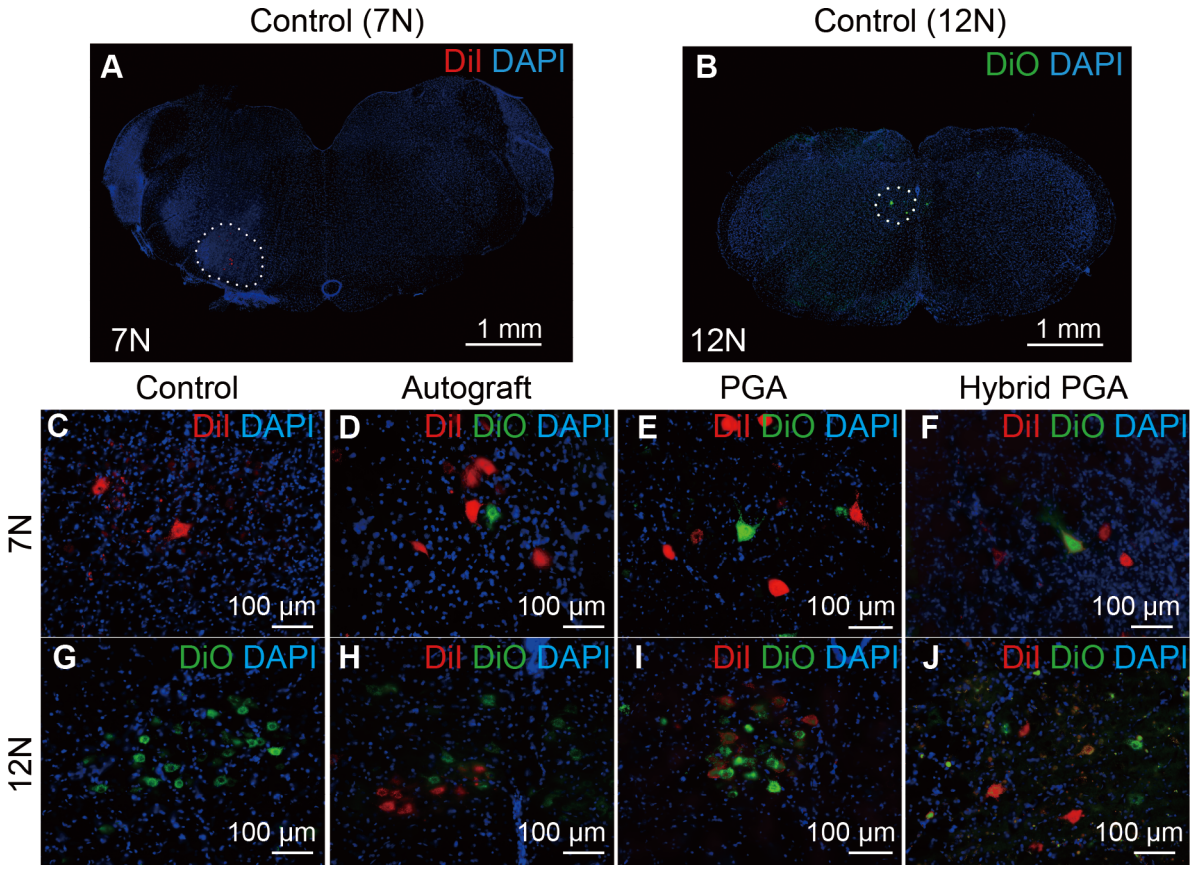

micr-18-0014-File010.tif